

## CONNECTIVITY ANALYSIS OF THE HABANERO ENHANCED GEOTHERMAL SYSTEM

Chaoshui XU<sup>1</sup>, Peter Alan DOWD<sup>1</sup>, Rosemarie MOHAIS<sup>1</sup>

<sup>1</sup>School of Civil, Environmental and Mining Engineering & South Australia Centre for Geothermal Energy Research, University of Adelaide, SA5005, cxu@civeng.adelaide.edu.au

### **ABSTRACT**

A realistic fracture model that adequately describes a fracture-stimulated reservoir is fundamental for subsequent flow and heat transfer analyses of the system. This paper describes a method to create such a model using seismic events recorded during the fracture stimulation process. The method is a Bayesian framework in the form of Markov Chain Monte Carlo (MCMC) simulation that effectively produces a fracture model conditioned by the seismic point cloud. The method is applied to Geodynamics' Habanero reservoir in the Cooper Basin of South Australia and detailed connectivity analysis between Habanero 1 and 3 is reported. The freeware FracSim3D is used for the analyses.

### **INTRODUCTION**

The understanding of connectivity between injection and production wells is critical in the design and performance assessment of enhanced geothermal systems (EGS). The connectivity depends largely on the fracture network of the reservoir. The realistic modelling of the network is still a very challenging problem due to the lack of meaningful measurement or relevant information. As a result, the only way to construct the fracture model for the reservoir is via a stochastic process. Stochastic fracture modelling is a general approach in which locations, size, orientation and other properties of fractures are treated as random variables with inferred probability distributions. In the simplest case, once the parameters of the distributions are inferred, the fracture model is constructed by Monte Carlo simulation (Xu and Dowd, 2010). First, the fracture locations are generated usually by a Poisson distribution in which fracture intensity for a particular area is either assumed to be constant or is derived from geostatistical estimation or simulation. Secondly, the orientation of each fracture is generated, most commonly from a Fisher distribution. Finally, the size of each fracture is generated from a specified distribution, the most common being exponential, lognormal or gamma. Other fracture properties, such as aperture width and

surface roughness, can then be added to the network by additional Monte Carlo steps. Options for fracture intersections and fracture termination can also be incorporated. Simulated fracture models are usually validated by sampling the model (using scan lines or areas on cross-sections) and assessing the extent to which the sampled values conform to the statistical models derived directly from survey data (Kulatilake *et al.*, 2003). In HDR EGS, however, this validation approach is of very limited value as only downhole surveys are possible and these can only record very limited information about the fracture density and orientation near the wellbores.

Major fluid conducting fractures in EGS are created by fracture stimulations. During the fracture stimulation process, two surfaces of existing fractures can slip against each other due to the reduction in effective normal stress acting across the fractures; the misalignment of surface profiles results in dilation and hence increases the permeability of the fractures. New fractures can also be created during the stimulation process if the hydraulic pressure is high enough to overcome the minimum in-situ compressive stress. The final product of the stimulation is an engineered geothermal system (EGS), or reservoir, through which the geothermal fluid will pass for heat extraction. Slip between fracture surfaces or fracture initiation/propagation will produce micro-seismicity that can be detected by an array of geophones, from which the locations of events can be determined. It is then reasonable to assume at least one fracture passes through any seismic event point, which forms the basis of the method reported in this paper. The inversion process (and associated accuracy issues) for deriving the hypocentres of the seismic events is not within the scope of the work reported here. .

### **HABANERO WELLS**

Habanero 1 (H1), drilled in 2003, was the first well in the Geodynamics' geothermal project in the Cooper Basin of South Australia. It was designed to become the injector for the future pilot plant. The depth of the well is 4421 m, 753 m into the basement rock and the temperature at the bottom of the well is close to 250°C with reservoir pressure at approximately 35

MPa above hydrostatic (Weidler 2005). The injectivity of the natural reservoir has been found to be around  $1 \text{ l.MPa}^{-1}.\text{s}^{-1}$  by the hydraulic test conducted at the completion of the well.

To create an effective fractured reservoir for efficient heat exchange, a fracture stimulation programme was conducted in November of 2003. Prior to the major stimulation programme, a fracture initiation phase consisting of three injection batches was designed for the purpose of opening up multiple fractures to maximize the effects of fracture stimulation. A total volume of  $1700 \text{ m}^3$  of water was injected at pumping pressure up to 69 MPa with peak pumping rate of  $63 \text{ l.s}^{-1}$ . However, most of the injected water was lost through the existing fracture zone at around 4255m below the surface.

The major fracture stimulation was run for about 11 days with a total of 13 million litres of water injected. It is believed that the existing fracture zone at a depth of 4255m attracts most of the hydraulic stimulation energy and hence this zone coincides with the fracture propagation (stimulation) zone that covers an area of roughly  $2.5 \text{ km}^2$  with a vertical extension of roughly 200m (Baisch et al 2006).

Eight geophones deployed in wells at depths ranging from 100m to 2300m were used to record the seismic events generated by the stimulation process. A total number of 23,232 seismic events were identified during the entire fracture stimulation period, including the fracture initiation phase and the post-stimulation injection tests (Figure 1) and their absolute hypocentres are shown in Figure 2. This dataset is used in this paper to demonstrate the analysis of connectivity between wells.

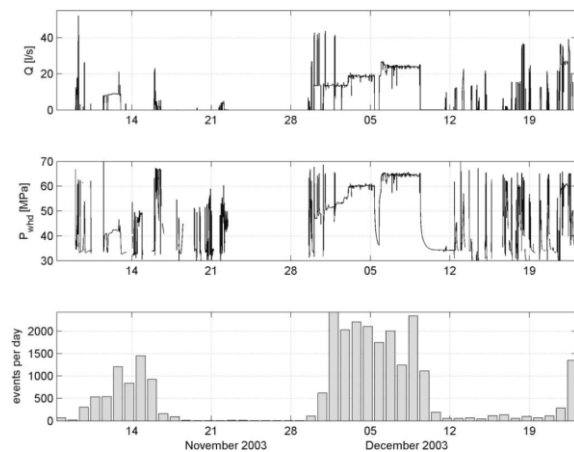


Fig. 1 Fracture stimulation history of Habanero 1 (Baisch et al. 2006)

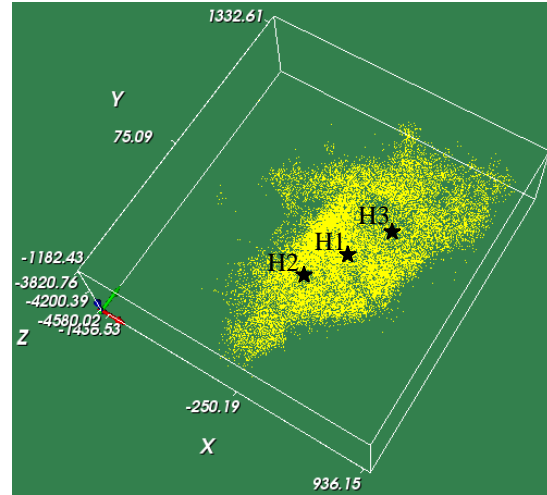


Fig. 2 Absolute hypocentre locations of the seismic events

Based on the initial assessment of the seismic event cloud, Habanero 2 (H2) was drilled in 2004 about 500m south-west of Habanero 1. Due to collar failure, about 245m of drill string was lost and a sidetrack was drilled to complete the well to a depth of 4358m. The sidetrack intersected the fractured reservoir at a depth close to prediction. A blockage in Habanero 2 in 2005 resulted in the loss of the well despite various attempts to by-pass the blockage. Habanero 3 (H3), with a larger diameter of  $8\frac{1}{2}''$  at the bottom of the well, was drilled in 2007 about 600m north-east of Habanero 1. The well was completed at a depth of 4221m.

### HABANERO RESERVOIR FLOW MODELLING

The characterisation of rock fracture networks, such as that for the Habanero reservoir, is a very difficult problem not least because accurate field measurement of a single fracture is difficult and measurement of all fractures is impossible. The only information available for the construction of a realistic fracture model is limited to borehole logging images and the sparse seismic events recorded over a large area of the reservoir. Because of the scale of the difficulty, the existing approaches for geothermal reservoir flow modelling either take a very simplistic view of the fracture network or use an equivalent porous media approach. For example, Zhang et al. (2009) use a penny-shaped fracture to represent the whole reservoir for their fluid and thermal flow analysis. Q-con (Vörös and Weidler 2006) uses a geological model that consists of a single fracture plus a permeable zone around the fracture termed the cataclastic zone. Xing et al. (2009) use an equivalent porous media approach derived from the seismic point cloud.

We take the view that these approaches are too simplistic to represent the reality of the fracture reservoir in Habanero. Earlier analyses of the seismic events conclude that the reservoir is probably dominated by some major sub-horizontal fractures, which agree well with the borehole logging images and the geometrical extent of the seismic point cloud. The vertical extent of the point cloud covers a band of nearly 500m in thickness and the highly concentrated region is approximately 300m (Fig. 1). Under this argument, a single fracture does not provide an adequate representation of the complexity of the reservoir.

### **CONSTRUCTION OF A REALISTIC FRACTURE MODEL**

The problem is to construct a fracture model conditioned to the seismic events under the assumption that at least one fracture passes through a seismic event point, i.e., an accurately conditioned fracture model should intersect all seismic event locations. This essentially becomes a stochastic geometry reconstruction problem given a set of point clouds. Reconstruction of a surface from random point clouds is computationally and algorithmically challenging and is an active research area in computer and mathematical sciences (Bercovier et al. 2002). The success of current practice, however, depends critically on close sampling points on the surface, which is usually not an issue as the point clouds are generally obtained from laser scanning or some form of digitizing. For seismic point clouds in geothermal applications, however, samples are very sparse. For a given fracture, only a few points are available, indicating either the propagation front of the fracture or a point on the fracture surface where shear slip occurs at the time the events are detected. Current methodology is thus not directly applicable to fracture modelling.

In reality, fracture planes are highly tortuous. It is impossible to represent all fractures by tortuous surfaces using a reasonable number of parameters and some simplification is required. The most common approach in stochastic fracture modelling is to use a 3D plane to represent a fracture, which could be bounded (e.g., elliptical plane, polygonal plane) or unbounded (e.g., Poisson plane). The validity of this representation is based on the assumption that fracture planes in the fitted model will follow closely the actual tortuous surfaces of the fractures in the reservoir or, in other words, the fitted fracture model is the first order approximation of reality. Within this framework, even the “best” fitted model will not intersect all seismic points but the distance of the points to fracture planes can be used as a criterion to assess the goodness-of-fit of the fracture model. The fracture model (network) then becomes a series of

connected fracture planes,  $F_i$ ,  $i=1,2,\dots,n$ , where  $n$  is the total number of fractures. A seismic event point,  $P_j$ ,  $j=1,2,\dots,m$  ( $m$  is the total number of seismic event points) can then be associated with a fracture  $F_i$  with distance  $d_{ji}$ . Because of the first order approximation of the fracture model, the complete set of projection distances  $d = \{d_{ji}\} \forall j$  will exhibit random variation from the fitted fracture planes. A Gaussian model is the most appropriate statistical model to describe random variation, or noise, from a first order approximation, i.e.,  $d_{ji} \sim N(0, \sigma^2)$ , where  $\sigma^2$  measures the degree of tortuous variability of fracture surfaces. The likelihood for the set of seismic event points  $P=\{P_j\}$  given a set of fitted fractures  $F=\{F_i\}$  can then be defined as:

$$f(\{d_{ji}\} | \theta) = \prod_{j=1}^m f(d_{ji} | \theta) = \left( \frac{1}{\sqrt{2\pi}\sigma} \right)^m \prod_{j=1}^m e^{-\frac{(d_{ji})^2}{2\sigma^2}} \quad (1)$$

with the set of parameters  $\theta = \{(x_i, y_i, z_i, \alpha_i, \beta_i, \gamma_i, a_i, b_i)\}$ ,  $i=1,2,\dots,n$ , where  $(x_i, y_i, z_i)$  are coordinates of the centre of fracture plane  $i$ ,  $(a_i, b_i)$  are the major and the minor axes of the ellipse containing the fracture polygon,  $(\alpha_i, \beta_i)$  are dip direction and dip angle of the fracture plane and  $\gamma_i$  is the rotation angle of the major axis of the ellipse against the dip direction of the fracture plane. The product of this likelihood with priors of  $F$  gives the posterior distribution for  $F$  and the attention now is to estimate the posterior distributions of  $F$  and hence the parameters of the fracture set. A Markov chain can be used to generate samples from the posterior distribution, which is commonly constructed by the Metropolis-Hastings algorithm using the Monte Carlo acceptance/rejection technique imposed by the Hastings' ratio (Gamerman (2006). For more detailed description of this algorithm, users are referred to Mardia *et al.* (2007), Xu et al. (2010, 2011).

### **HABANERO FRACTURE MODEL**

Baisch *et al.* (2006) use cross-correlation coefficients between waveforms to group the seismic events and they identify 613 clusters of events using the criterion of coefficients  $> 0.85$ . A total of 9,176 events are included in these clusters with the number of events in a cluster ranging from 2 to 158. Planes are then fitted to these clusters to improve the geometrical reservoir model. To mimic the fittings of these clusters, a fracture model consisting of 613 fractures using the following priors was generated:

- Fracture orientation: Fisher distribution with  $\kappa=1$ . Orientation parameters  $(\alpha_i, \beta_i, \gamma_i)$  are then calculated.
- Fracture size: lognormal distribution with mean = 80 m and variance = 12,000 m<sup>2</sup>.

The MCMC algorithm described above is then used to optimise the fracture network by following a chain of Markov samples aiming to maximize the

likelihood function given in Eq. 1. The initial fracture model is shown in Figure 3. The fracture model after a million MCMC steps is given in Figure 4. For this model, numbers of seismic events associated with fracture planes range from 1 to 394. Figure 5 shows the projection of fitted fracture plane 286 where it has 394 associated seismic points.

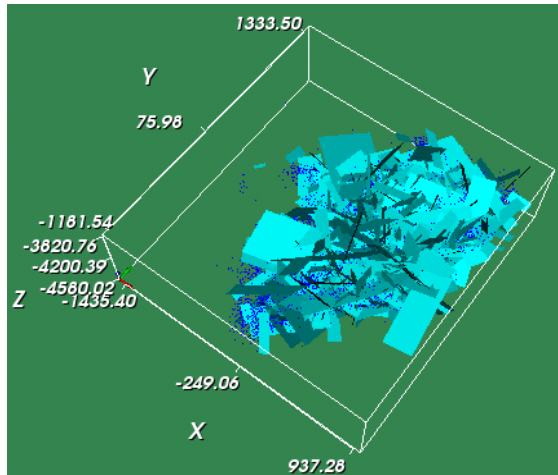


Fig. 3 Initial Habanero fracture model

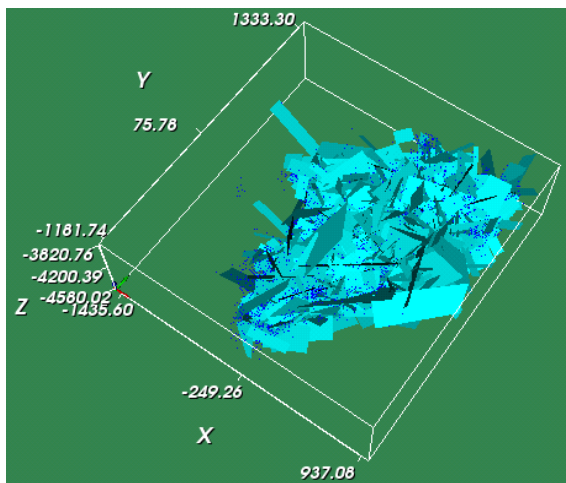


Fig. 4 Habanero fracture model after optimisation

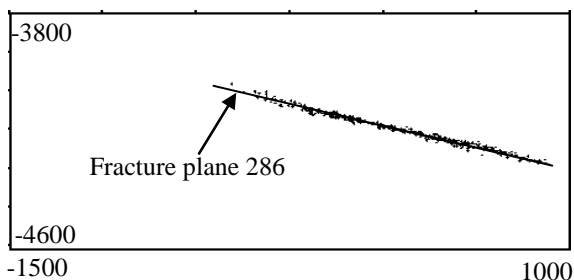


Fig. 5 Fitted fracture plane 286 (NB: vertical axis is exaggerated to give a clearer view of the point distribution)

The distribution of  $d=\{d_{j,i}\}\forall j$  is given in Figure 5a. It is interesting to compare this distribution with the histogram of distances of relative hypocentre locations to layers determined separately for each cluster shown in Fig. 11 in Baisch *et al.* (2006) where 95 percent of the relative hypocentre locations are within  $\pm 25$  m (estimated) from the layers. For the MCMC fracture model, this number is  $\pm 12$  m, which indicates that the MCMC fracture model is a better fit. This is remarkable considering that no waveform correlation analysis is required and the difficulty of the model fitting was increased by taking into account all 23,232 seismic events while the model in Baisch *et al.* (2006) is based on only 9,176 events. This also raises a concern about the assumption that seismic events with high cross-correlation coefficients belong to the same fracture (cluster) (Xu *et al.*, 2011, Moriya *et al.* 2002).

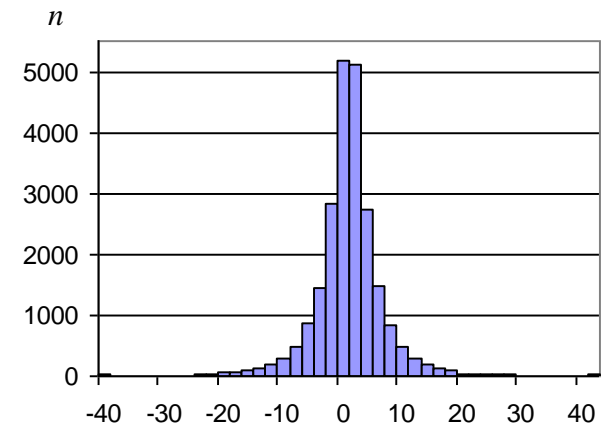


Fig. 6 Distribution of  $d_{j,i}$

It is also interesting to examine the orientations of the fitted fracture planes. Figures 7 and 8 give the pole projections of 613 fractures before and after the MCMC optimisation. Figure 7 is essentially the orientation distribution of the prior fracture model which shows a high degree of randomness. After optimisation (Figure 8), many fracture planes become sub-horizontal. This result agrees well with the analysis done by Baisch *et al.* (2006) where fitted planes of 203 clusters (out of 613) were shown to have a dip angle less than  $30^\circ$ .

### CONNECTIVITY ANALYSIS

Fracture network connectivity is an important issue in EGS modelling as it largely determines the flow characteristics of the reservoir. However, finding channels connecting injection and production wells through a fracture network is by no means simple. To demonstrate the complexity of the problem, the fracture model fitted by the MCMC process is used to analyse the connectivity between the Habanero 1 (H1) and 3 (H3) wells. For the fracture model with 613 fractures, there is a total of 27,293 possible

connection channels through the fracture network between the two wells. These paths are depicted in Figure 9 and their statistics are given in Figure 10 and 11. Clearly Habanero 1 is well-connected to its surrounding rock through the fracture model, which is expected because of the fracture stimulation.

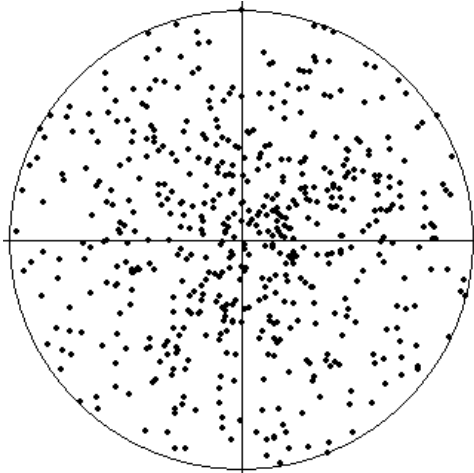


Fig. 7 Pole projections of 613 fracture planes (initial fracture model)

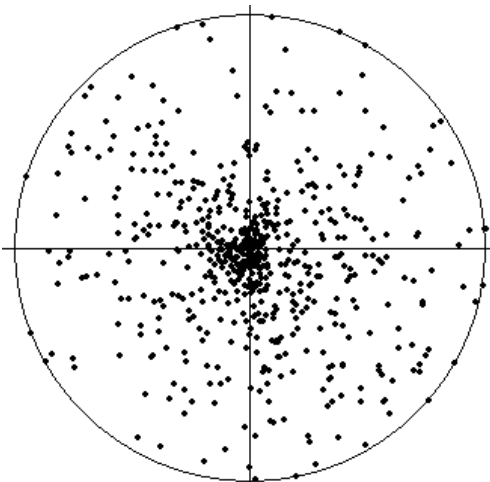


Fig. 8 Pole projections of 613 fracture planes (optimised fracture model)

There are only a few connection paths between Habanero 3 and the fracture model, which is also expected as Habanero 3 plays no part in the fracture stimulation process described in this paper. It is interesting to note that for the initial fracture model, there is only a total number of 9,135 connection paths between H1 and H3, which is about a third of that of the optimised model. This demonstrates that the optimised model fits much better to the actual fracture network as a significantly improved connectivity of the reservoir is expected after the fracture stimulation. Another interesting point to note is that there is a significant increase in smaller distance paths connecting the two wells (an increase

from 5% to 9% for distance less than 4km, see the histograms in Fig. 10 where the solid line is for the optimised fracture model and the broken line is for the original model). This suggests the optimised model has more sub-horizontal fractures hence causing the connection paths between the two wells to be shortened. There are 103 connection paths in the optimised fracture model with distances less than 1km while for the original fracture model there are only 20. The smallest connection path distance in the optimised model is 609 m while in the original model it is 758 m. There are also five connection paths in the optimised model that only pass through two nearly parallel fractures. These results demonstrate further that the MCMC process works well. It is also remarkable that the majority of connection paths are over 10 km, given that the direct distance between the two wells is only 586 m. Most of these connection paths pass through more than 100 fracture planes (Figure 11).

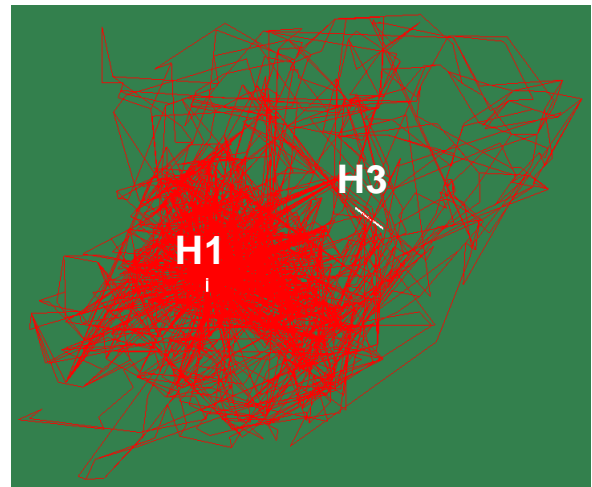


Fig. 9 Connection channels between Habanero 1 & 3

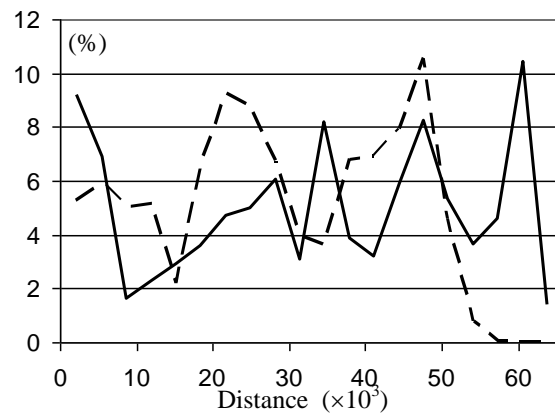


Fig. 10 Histogram of distances of connection paths



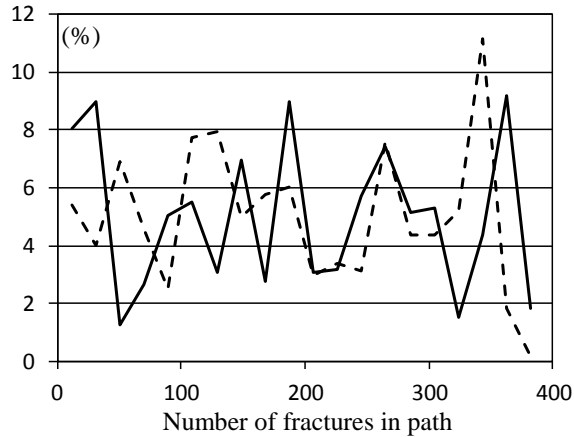


Fig. 11 Histogram of number of fractures passed through by connection paths

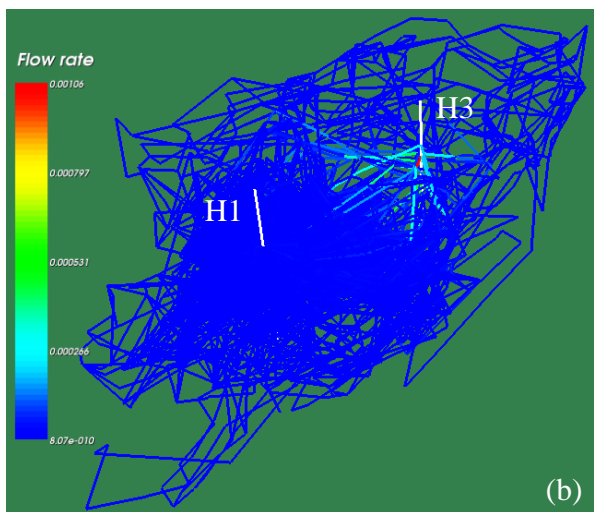
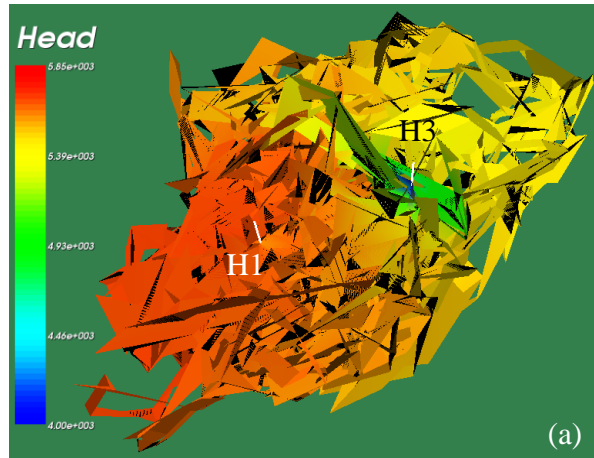


Fig. 12 Flow simulation using equivalent pipe model approach, (a). total head in mH<sub>2</sub>O, (b). flow rate in m<sup>3</sup>/s.

Once all the connection paths between the two wells have been identified, some preliminary assessment of the flow characteristics of the reservoir can be performed using a pipe model approach (Dershowitz and Fidelibus 1999). Figure 12 shows the evaluation results for such a model. In this analysis, the pressure head difference between the two wells is kept at 15 MPa and a constant fracture aperture of 100  $\mu\text{m}$  is used for the fracture model. Two important observations can be made:

- Although there is a large number of channels connecting the two wells, most of the flow is through only a few of them and the flow through the majority of connection paths is almost negligible. It is important to identify these major flow channels and connectivity analysis provides a means of doing so.
- Shorter paths do not necessarily have higher hydraulic conductivity as conductivity also depends on the lengths of intersections between fractures that make up the connection paths. This is evident in Figure 13. The statistical analysis of fracture intersection lengths (Figure 13) is given in Figure 14.

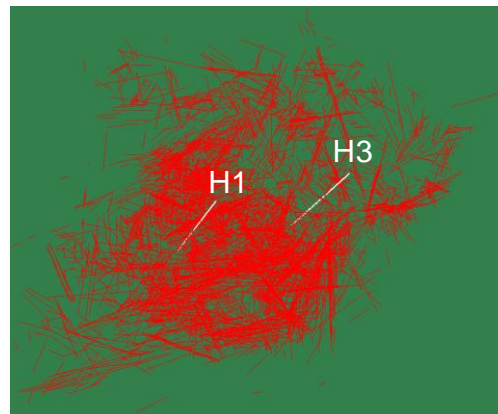


Fig. 13 Fracture intersection lines of Habanero fracture model

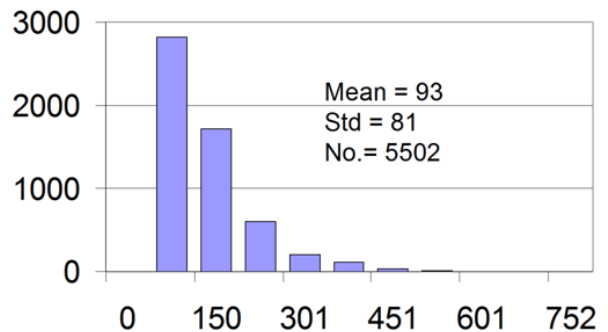


Fig. 14 Statistics of fracture intersection lines

Figure 12 should be compared to Figure 15 where the flow simulation is done on the initial fracture model. Using a constant hydraulic aperture of  $100\ \mu\text{m}$  for both fracture models and  $10^{-6}\ \text{m}^2\cdot\text{s}^{-1}$  as the kinematic viscosity for the fluid, the flow rate achieved in the original and the optimised model are  $1.6\ \text{l}\cdot\text{s}^{-1}$  and  $5.9\ \text{l}\cdot\text{s}^{-1}$ , which is almost a four fold increment. These correspond to the reservoir impedance of  $9.4\ \text{MPa}\cdot\text{l}^{-1}\cdot\text{s}^{-1}$  and  $2.5\ \text{MPa}\cdot\text{l}^{-1}\cdot\text{s}^{-1}$  respectively. Clearly the optimised model reflects much better the actual connectivity of the reservoir due to the stimulation.

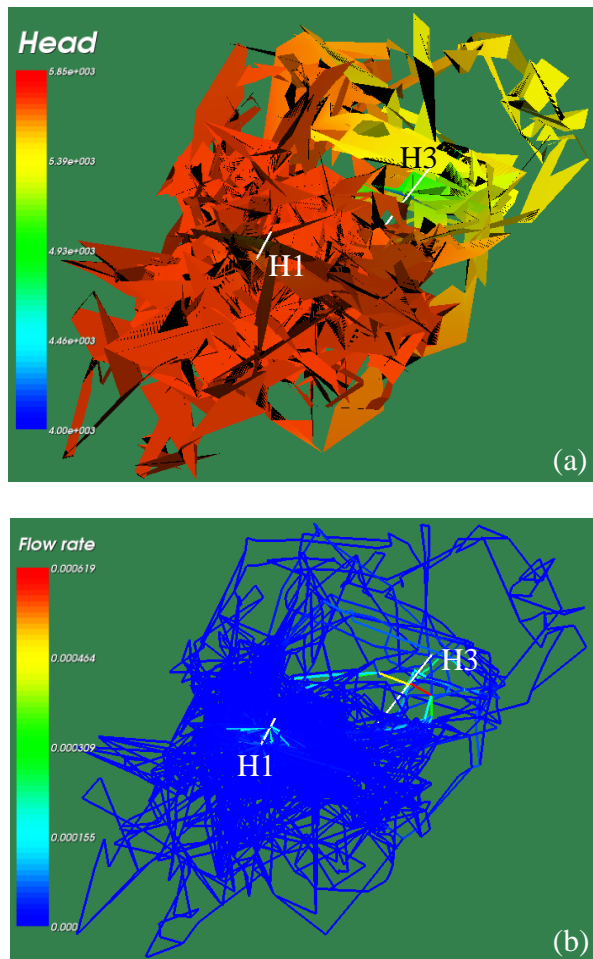


Fig. 12 Flow simulation using equivalent pipe model approach, (a). total head in  $\text{mH}_2\text{O}$ , (b). flow rate in  $\text{m}^3\cdot\text{s}^{-1}$ .

## CONCLUSIONS

MCMC has been demonstrated to produce remarkably good results for fitting an optimised fracture model according to the specified criterion, both at the global scale and at the scale of an individual fracture. The model also confirms the sub-

horizontal features of fractures observed in the Habanero reservoir.

Connectivity is an important fracture network property for the assessment of fluid flow and heat transfer characteristics of EGS. The evaluation of connectivity between wells is extremely complex even for a fracture model of modest size, as demonstrated for the Habanero reservoir.

The work reported here demonstrates the effectiveness of using MCMC for fracture model conditioning by seismic events. It also describes subsequent connectivity analysis of the fracture model for the Habanero reservoir. The seismic data used in this study are from the fracture stimulation of Habanero 1 in 2003. Since then, Geodynamics has performed further stimulations in the area. The new datasets, however, were not incorporated in the model described here.

## ACKNOWLEDGEMENT

We thank Geodynamics Limited for allowing access to microseismic data and for its review of the paper.

## REFERENCES

- Baisch, S, Weidler, R, Vörös, R, Wyborn, D and de Graaf, L, 2006. Induced seismicity during the stimulation of a geothermal HFR reservoir in the Cooper Basin, Australia, *Bulletin of the Seismological Society of America*, 96 (6): 2242–2256.
- Baisch, S, Vörös, R, Weidler, R and Wyborn, D, 2009. Investigation of fault mechanisms during geothermal reservoir stimulation experiments in the Cooper Basin, Australia, *Bulletin of the Seismological Society of America*, 99 (1): 148–158.
- Dershowitz, W. S. & Fidelibus, C. 1999, Derivation of equivalent pipe network analogues for three-dimensional discrete fracture networks by boundary element method, *Water Res. Research*, 35 (9), 2685–2691.
- Gamerman, D, 2006. *Markov Chain Monte Carlo: stochastic simulation for Bayesian inference* (2<sup>nd</sup> ed) (Chapman and Hall/CRC).
- Mardia, K V, Nyirongo, V B, Walder, A N, Xu, C, Dowd, P A, Fowell, R J and Kent, J T, 2007. Markov Chain Monte Carlo implementation of rock fracture modelling, *Mathematical Geology*, 39: 355 – 381.
- Moriya, H, Nakazato, K, Niitsuma, H and Baria, R, 2002. Detailed fracture system of the Soultz-sous-Forêts HDR field evaluated using microseismic multiplet analysis, *Pure and Applied Geophysics*,

159: 17-541. Weidler, R., 2005. The Cooper Basin HFR project 2003/2004: findings, achievements and implications, Technical report, Geodynamics Ltd.

Vörös, R. and Weidler, R. (Q-con GmbH, 2006) Numerical thermo-hydraulic simulation of a large scale power production in the Cooper Basin, Technical Report GDY018, Geodynamics.

Weidler, R. (2005) The Cooper Basin HFR Project 2003/2004: Findings, achievements and implications, Technical Report, Geodynamics Ltd.

Xing, H., Zhang, J., Liu, Y. and Mulhaus, H. (University of Queensland, 2009) Enhanced geothermal reservoir simulation, *Proceedings of the Australian Geothermal Energy Conference 2009*, Brisbane.

Xu, C and Dowd, P A, 2010. A new computer code for discrete fracture network modelling, *Comps & Geosc.*, 36: 292-301.

Xu, C, Dowd, P A and Wyborn, D, 2010. Optimised fracture model for Habanero reservoir, in *Proceedings of the Australian Geothermal Conference 2010* (Geoscience Australia: Adelaide).

Xu, C, Dowd, P A and Wyborn, D, 2011. Optimisation of a stochastic rock fracture model using Markov Chain Monte Carlo Simulation, *Proceedings of the 35th International Symposium on the Application of Computers and Operations Research in the Minerals Industries (APCOM2011)*, Wollongong, Australia, 2011.

Zhang, X. Jeffrey, R. and Wu, B. (CSIRO, 2009) Two basic problems for hot dry rock reservoir stimulation and production, *Proceedings of the Australian Geothermal Energy Conference 2009*, Brisbane.